Available online at www.sciencedirect.com
SCIENCE DIRECT®
Diamond and Related Materials 12 (2003) 499–502
DIAMOND AND RELATED MATERIALS
www.elsevier.com/locate/diamond

Carrier dynamics in CVD diamond: electron and hole contributions

Cristina Tuvè[a,b,*], V. Bellini[a,b], R. Potenza[a,b], C. Randieri[a,b], C. Sutera[a,b], G. Pucella[c], M. Marinelli[c], E. Milani[c], A. Paoletti[c], A. Tucciarone[c], G. Verona-Rinati[c]

[a]*Università di Catania, Corso Italia 57, I-91124 Catania, Italy*
[b]*INFN – Sezione Catania, Corso Italia 57, I-91124 Catania, Italy*
[c]*INFM – Dipartimento di Ingegneria Meccanica, Università di Roma 'Tor Vergata', Via di Tor Vergata 110, I-00133 Rome, Italy*

Abstract

The transport properties in synthetic diamond are studied using high quality diamond films grown by microwave plasma enhanced chemical vapor deposition (CVD). In particular, electron and hole contributions to the diamond carrier dynamics are successfully separated and defect distribution inside specimens is obtained. This is achieved through a systematic investigation of the signals obtained from properly biased diamonds irradiated with differently penetrating nuclear particles. To this purpose ^{12}C ions produced by the 15 MV Tandem accelerator of the Southern National Laboratories of INFN in Catania (Italy) are used as a probe. The ion beam energy is varied in the 22–91 MeV range (penetration depth from 10.5 μm to the thickness of the used samples, deposited energies from 22 to 62 MeV and mean energy densities from 0.8 to 2.1 MeV/μm, respectively). The sample responses are studied as a function of the ^{12}C energy and penetration depth, both in the positive and negative bias polarization. The experimental results clearly show that, when the detector is previously driven in the so-called pumped state by ^{90}Sr β-particle irradiation, a different behavior of signals is observed in the positive and negative polarization states. The data are analysed in the framework of a properly modified Hecht model were the different behavior of carriers and influence of the variation in the ionization density along the path of the incident particles are considered. As a novelty the inhomogeneous distribution of defects is taken into account. By fitting the experimental curves with the model, a quantitative estimate of the defects distribution and of the correlated mean drift distance for electron and holes can be obtained. A good agreement is observed, thus allowing a better understanding of the diamond growth.

Keywords: Diamond production; Diamond properties and applications; CVD; Defects; Modeling

1. Introduction

Diamond was shown to be a suitable material for applications in high energy particle detection [1] due to its striking electronic properties, such as a high carrier mobility, wide band-gap, good radiation hardness and very high breakdown voltage. Recently very high quality diamond films could be deposited by microwave plasma enhanced chemical vapor deposition (CVD), whose properties result to be even better than in natural single crystal diamond with respect to several applications. However, the polycrystalline nature of CVD diamond and the presence in it of a high concentration of crystallographic defects still constitute a severe limitation to most of the technological applications [2].

As far as the feasibility of a diamond-based high energy particle detector is concerned, two main properties are of interest, namely the average charge collection distance δ and the detector efficiency η, defined as follows. An ionizing particle impinging on a parallel plate detector of thickness *L*, creates a number of electron–hole pairs. As a consequence, in the presence of an external applied filed *E*, a charge is induced per each pair in the electric circuit $q_c = ex/L$, *x* being the total distance the electron and hole move apart [3]. The average charge collection distance is then:

$$\delta = \lambda_e + \lambda_h = (\mu_e \tau_e + \mu_h \tau_h) E \quad (1)$$

where μ_e, μ_h, τ_e and τ_h are mobilities and lifetimes of electrons and holes, respectively. The detector efficiency η is given by the ratio between the collected charge

*Corresponding author. Tel.: +39-34952131922; fax: +39-34952132382.
E-mail address: cristina.tuve@ct.infn.it (C. Tuvè).

0925-9635/03/$ - see front matter © 2003 Elsevier Science B.V. All rights reserved.
doi:10.1016/S0925-9635(02)00390-4

Q_c and the total charge generated by the incident ionizing particle Q_0:

$$\eta = Q_c/Q_0 \tag{2}$$

If we assume different drift mean path for the two carriers and constant distribution for the ionizing particle from 0 to the penetration depth G, we obtain the simplest extension of the Hecht formula [4]:

$$\eta = \frac{\lambda_e + \lambda_h}{L} - \frac{\lambda_e^2(1 - e^{-G/\lambda_e}) + \lambda_h^2(e^{-(L-G)/\lambda_h} - e^{-L/\lambda_h})}{LG} \tag{3}$$

where a uniform electric field E is assumed.

Measurements with α-particles from ^{241}Am showed in the pumped state a different behavior of electrons and holes [5]. However that experiment was not sensitive to the variation of ionization density (the Bragg function) and to the spatial defect distribution. In this paper we perform new measurements using ^{12}C energetic beams from the 15 MV Tandem accelerator of the Southern National Laboratories (LNS) of INFN in Catania (Italy) to investigate in detail the behavior of CVD diamond films in different respects: ^{12}C ions seem very suitable for this investigation due to the possibility of varying penetration depths and ionization density within large limits (which is impossible to do with α-particles), allowing to give insight on the spatial defect distribution. We report here preliminary results of this new approach, based on measurements on a limited number of samples. In spite of this limitation, significant features of the defect distribution are already brought into light.

2. Experimental

Detector grade CVD diamond films were grown on single crystal (1 0 0) p-type silicon substrates using a CH_4–H_2 gas mixture in a tubular reactor properly modified to improve the crystal quality [6]. The usual scratching procedure was adopted to promote nucleation. The CH_4 content in the gas fed and the substrate temperature during the deposition process were fixed to 1% and 750 °C, respectively, so that a growth rate of approximately 0.7 μm/h was obtained. Two detectors (labeled as D1 and D2) were obtained by depositing Au contacts 7 mm^2 wide and 100 nm thick on two different diamond samples deposited in two different growth reactors. Both D1 and D2 are ≈55 μm thick. A 60 h irradiation with β-particles from a ^{90}Sr source was made as the standard procedure to drive the detectors in the fully pumped state.

In the previous experiments with α-particles [5], the penetration depth varied from 1.7 up to 13.7 μm, starting from the growth surface, and energies from 1 to 5.5 MeV. An interesting feature that was observed is the asymmetric behavior when the sample is driven in the two different bias polarities: the efficiency for positive bias is greater then for the negative one. This behavior is well explained assuming that the mean drift distance for holes is much greater than for electrons: $\lambda_h \gg \lambda_e$. Precisely, being the penetration depth of the α-particles much lower than the thickness of the sample, the carriers are generated in the region near the growth surface. Then, for positive bias the holes can travel for most of the sample generating an high signal (we define 'positive' the voltage supply when the growth side of the diamond, normally that with less defects, is driven by positive voltage, 'negative' the reverse one). For negative bias the drift distance of holes is limited by the electrode contact. The corresponding electrode contact limitation for electrons, in case of positive bias, is smaller due to their lower mean drift distance.

Because the maximum penetration depth of the α-particles is much lower than the thickness of the sample, it seemed worthwhile to perform new measurements using as probe ^{12}C beam in order to allow a large range of the penetration depth inside the diamond detector.

For the tests under ion bombardment a ^{12}C beam produced at the Tandem accelerator of the INFN Catania Laboratories was used. The energy of ^{12}C particles was varied in steps between 22.0 and 91.2 MeV. The intensity of the beam varied between 2 and 10 pnA (that is between 1.25×10^{10} and 6.25×10^{10} particles/s). The beam impinged onto a gold target 150 μg/cm^2 thick and the diamonds detected the particles scattered at angles 10 or 20°. The detectors were approximately 50 μm thick, so that ^{12}C particles of energy higher than 60 MeV penetrated along the whole thickness loosing only part of their energy, while particles with lower energies lost all the energy, but penetrated only part of the thickness. ^{12}C penetration depths varied from 10.5 μm to the thickness of the used samples, deposited energies from 22 to 62 MeV and mean ionization energy densities from 0.8 to 2.1 MeV/μm, respectively. Tests were performed for positive and negative polarization of diamonds. The absolute value of the voltage was such to produce a field $E = 1$ V/μm $= 10$ kV/cm.

During all the tests the pulses produced in the diamonds were amplified by conventional analogic methods, digitalized through ADC's and stored.

3. Results and discussion

We refer here about the new measurements under ^{12}C bombardment on two diamond detectors. Figs. 1 and 2 show the efficiency η (Eq. (2)) for D1 and D2, respectively, as a function of the ^{12}C energy. The beam impinged on the growth side in all cases. As we can see, all diamonds under test show similar trends for the

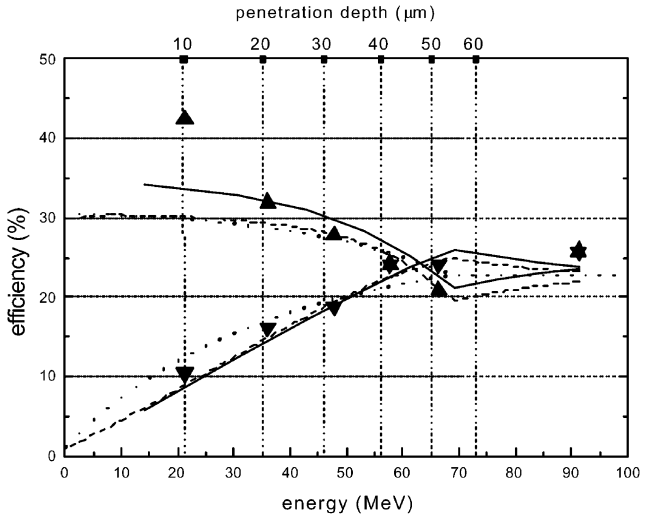

Fig. 1. Efficiency in charge collection of D1 bombarded with ^{12}C at various energies. The penetration depths of ^{12}C particles are also shown. See text for the explanation of the theoretical curves. The constants in the distribution of defects for the computation of full-length curve were: $a_e = 1.25/\mu m$, $a_h = 0.03/\mu m$, $b = 0.036/\mu m$ and $c = 37$ μm.

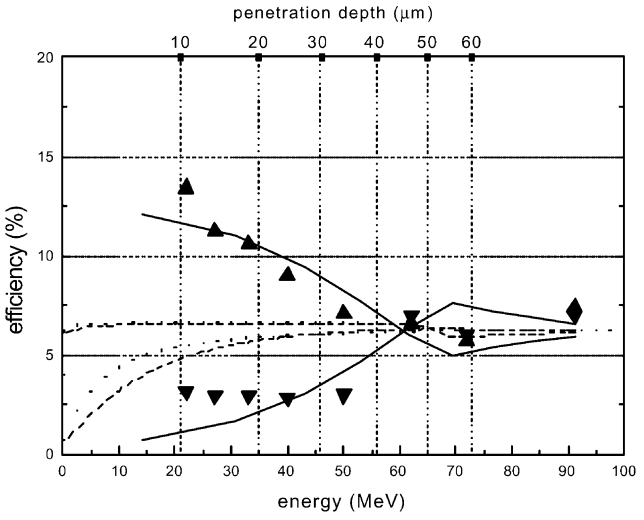

Fig. 2. As in Fig. 1 for D2; constants were: $a_e = 3.3/\mu m$, $a_h = 0.13/\mu m$, $b = 2.86/\mu m$ and $c = 8$ μm.

efficiency, but D2 shows a lower efficiency than D1 at all beam energies.

The first calculations of the efficiencies done with the simple model (Eq. (3)) are reported as dotted line in the figures. As we can see, these lines fit well the data for the D1, especially at negative voltage, but the fit is not good for the low efficiency D2. Then we modified the above model, that assumed a constant distribution of ionizing density, by using the Bragg function, as calculated by a standard nuclear physics simulation program. The dashed lines in Figs. 1 and 2 refer to the model with the Bragg distribution. With this assumption it is possible to reproduce the curve-crossing at moderately high energy because in this energy range the charge is mostly generated near the interface. At higher energies the ^{12}C particles cross the sample and the released energy tends to be uniform and the detector response becomes the same for positive and negative bias.

As shown in Fig. 2, the introduction of the Bragg distribution does not allow to reproduce the behavior at low energy for the lower quality sample. At this point it seemed necessary to introduce the variations of the collection lengths. This can be made with the assumption that defects limiting the collection efficiency can be separated into in-grain defects and grain boundaries effect [7]. The in-grain defects, different for electrons and holes, are supposed uniform through the films thickness. The grain-boundaries effect is supposed to be the same for both carriers. As for the spatial distribution, a work hypothesis was made, following Ref. [7], reproducing the well known property that grain-boundaries defect density increases as one approaches the film–substrate interface: an exponential function was utilized. Thus the overall spatial distribution of defects was:

$$g_{e,h}(x) = a_{e,h} + be^{-x/c} \quad (4)$$

different of course for holes and electrons. In Eq. (4) the x-axis goes along the direction of the particle beam, from the nucleation surface of the diamond to the growing one. Eq. (4) brings to a variation of the charge collection lengths. Introducing these corrections into the model through the natural convolutions of Eq. (3), we obtained the solid lines reported in the figures.

The values of a_e, a_h, b and c used for the two diamonds are reported in Table 1.

As we can see, D1 shows a defect distribution essentially uniform and the response of the detector is mostly limited only by the in-grain defects. In the other case, defects appear mostly concentrated near the nucleation surface, showing the importance of a fine control of the reactor during the growth of the first few microns of carbon deposition.

Table 1

	D1	D2
a_e (1/μm)	1.25	3.3
a_h (1/μm)	0.03	0.13
b (1/μm)	0.036	2.86
c (μm)	37	8

4. Conclusions

Measurements with ^{12}C ions produced by Tandem of LNS, Catania, allow a large range of the penetration depth inside the diamond film. This technique permits to scan the detection properties of the whole sample thickness allowing to give new insight on the spatial defect distribution. This was done by taking into account an inhomogeneous spatial distribution of defects for both carrier types, in addition to the nonuniform ionization due to the incident nuclear particles.

We report preliminary results of this method. In particular, as detailed in the previous discussion, the importance of different growth conditions is brought into light, using a limited number of samples. These results show that the detection process of ^{12}C ions of different energies can be a powerful instrument to explore in detail diamond structure and to suggest improvements in careful engineering of the first stages of diamond growth.

References

[1] W. Adam, et al., Electrochemical Society, Fifth Symposium on Diamond Materials Proceedings (1998) 491.
[2] D.R. Kania, in: A. Paoletti, A. Tucciarone (Eds.), The Physics of Diamond, IOS Press, Amsterdam, 1997.
[3] S. Ramo, Proc. I.R.E. 27 (1939) 584.
[4] K. Hecht, Z. Phys. 77 (1932) 235.
[5] M. Marinelli, E. Milani, A. Paoletti, et al., Phys. Rev. B 64 (2001) 195205.
[6] M. Marinelli, E. Milani, A. Paoletti, et al., Proceedings of Applied Diamond Conference/Frontier Carbon Technology Joint Conference, Tsukuba, Japan, August 31–September 3, (1999) 154.
[7] M. Marinelli, E. Milani, A. Paoletti, et al., Appl. Phys. Lett. 75 (1999) 3216.